Journal of Engineering Mathematics **25**: 99–113, 1991.

Convection in a shallow laterally heated cavity with conducting boundaries

R.J. GARGARO

Department of Mathematics, City University, Northampton Square, London EC1V 0HB, UK

Received 13 November 1989; accepted in revised form 20 August 1990

Abstract. Shallow cavity flows driven by horizontal temperature gradients are analysed over a range of Rayleigh numbers R and Prandtl numbers σ, where R is comparable in size to the aspect ratio $L(\geqslant 1)$. Eigenvalue calculations show the existence of a critical Prandtl number σ_c, below which the parallel core-flow structure is destroyed for Rayleigh numbers $R > R_c(\sigma)$. For other Rayleigh numbers and Prandtl numbers the horizontal scale of influence of the end walls of the cavity is determined.

1. Introduction

Convective motions driven by temperature gradients not aligned with the gravitational field were first studied in connection with large-scale geophysical disturbances (Hadley [1]; Jeffreys [2]; Defant [3]; Stern [4]). The lateral extent of the flow is a key factor in many modern applications including certain crystal growing techniques (Hurle [5]; Hurle et al. [6]; Gill [7]), cooling systems for nuclear reactors (Boyack and Kearney [8]), dispersion of pollutants in river estuaries (Cormack et al. [9]), and in solar energy collectors (Bejan and Rossie [10]). Cavity flows driven by lateral heating have been investigated experimentally by Rossby [11], Imberger [12], Ostrach et al. [13], Bejan et al. [14], Simpkins and Dudderar [15] and Simpkins and Chen [16]. These flows driven by horizontal temperature gradients heat up the fluid near the hot wall causing it to rise and flow across the upper half of the cavity to the top of the cold wall. There it cools and descends to the bottom of the wall, and it then completes the circuit along the bottom half of the cavity. The movement of fluid around the cavity is achieved in such a way that there is an odd symmetry about the centre (Gill [17]). Numerical studies of this motion have been discussed by Quon [18], Cormack et al. [19], Shiralkar and Tien [20] and Kuo et al. [21]. At high Rayleigh numbers experiments in shallow cavities indicate that the central region of the core is almost stagnant (Bejan et al. [14], Simpkins and Chen [16], whilst vertical boundary layers at the ends of the cavity occasionally exhibit local internal eddies (Simpkins and Dudderar [15]). The core region is dominated by a horizontal shear flow for lower, although still large, Rayleigh numbers but this can be replaced by a multicellular structure if the Prandtl number of the fluid is small enough (Hart [22, 23], Gill [7]).

The present study is concerned with the basic steady flow in the cavity and with the solution near the vertical walls. The horizontal boundaries are assumed to be conducting. The companion problem for insulated boundaries has already been discussed by Daniels et al. [24]. The Rayleigh number R based on height (see (2.10) below) is $O(L)$, where $L(\geqslant 1)$ is the aspect ratio of the cavity, so that nonlinear effects are significant. The local solution near the vertical walls involves eigensolutions that generally decay away into the core region;

these eigensolutions are involved in turning the flow in the end region, but one is associated with a stationary transverse mode of instability (Hart [22, 23]) which can present itself at low Prandtl numbers. The parallel core flow is destroyed by this spatial oscillation, and as the Rayleigh number increases the instability is forced into the system as a smooth transition emanating from the ends of the cavity. This paper determines the range of Prandtl numbers and Rayleigh numbers for which this imperfect bifurcation occurs. It also determines the lateral extent of the end zones for general Prandtl numbers and Rayleigh numbers. A complete numerical solution of the end zone problem has not been attempted.

2. Formulation of the problem

The flow domain is a rectangular cavity of height h and length l. The end walls are maintained at fixed but different temperatures which generate steady two-dimensional motions within the cavity. The governing equations for the flow, taking buoyancy into consideration, are the Navier–Stokes equations,

$$u^* \frac{\partial u^*}{\partial x^*} + w^* \frac{\partial u^*}{\partial z^*} = -\frac{1}{\rho^*} \frac{\partial p^*}{\partial x} + \nu\left(\frac{\partial^2 u^*}{\partial x^{*2}} + \frac{\partial^2 u^*}{\partial z^{*2}}\right), \tag{2.1}$$

$$u^* \frac{\partial w^*}{\partial x^*} + w^* \frac{\partial w^*}{\partial z^*} = -\frac{1}{\rho^*} \frac{\partial p^*}{\partial z^*} + \nu\left(\frac{\partial^2 w^*}{\partial x^{*2}} + \frac{\partial^2 w^*}{\partial z^{*2}}\right) - g, \tag{2.2}$$

the heat equation,

$$u^* \frac{\partial T^*}{\partial x^*} + w^* \frac{\partial T^*}{\partial z^*} = \kappa\left(\frac{\partial^2 T^*}{\partial x^{*2}} + \frac{\partial^2 T^*}{\partial z^{*2}}\right), \tag{2.3}$$

and the continuity equation

$$\frac{\partial}{\partial x^*}(\rho^* u^*) + \frac{\partial}{\partial z^*}(\rho^* w^*) = 0, \tag{2.4}$$

where (x^*, z^*) are Cartesian co-ordinates, x^* in the direction along the horizontal boundaries and z^* in the direction up the end walls with the origin at the bottom of the cold wall ($x^* = 0$). u^* and w^* are the velocity components in the directions x^* and z^* respectively and T^* is the temperature with $T^* = T_0^*$ on the cold wall; p^* is the pressure, ρ^* is the density, ν is the kinematic viscosity, κ is the thermal diffusivity and g is the acceleration due to gravity.

It is assumed that

$$\rho^* = \rho_0(1 - \beta(T^* - T_0^*)), \tag{2.5}$$

where ρ_0 is the density at $T^* = T_0^*$ and β is the coefficient of thermal expansion. In line with the Oberbeck–Boussinesq approximation the variation of density with temperature is assumed to only affect the buoyancy term in (2.2). Introducing Cartesian co-ordinates $(\bar{x}, \bar{z})$ made dimensionless with respect to the height h, the stream function $\bar{\psi}$ made dimensionless with respect to the thermal diffusivity κ and the temperature $\bar{T}$ made dimensionless with respect to the temperature difference $\Delta T'$ applied between the two end walls, (2.1) to (2.4) can be rewritten as

$$\bar{\nabla}^4\bar{\psi} - R\frac{\partial \bar{T}}{\partial \bar{x}} = \frac{1}{\sigma}\frac{\partial(\bar{\nabla}^2\bar{\psi}, \bar{\psi})}{\partial(\bar{x}, \bar{z})}\,, \tag{2.6}$$

$$\bar{\nabla}^2\bar{T} = \frac{\partial(\bar{T}, \bar{\psi})}{\partial(\bar{x}, \bar{z})}\,, \tag{2.7}$$

where $\bar{\nabla}^2$ is the Laplacian operator. Here the pressure has been eliminated and

$$\bar{u} = \frac{\partial \bar{\psi}}{\partial \bar{z}}\,, \qquad \bar{w} = -\frac{\partial \bar{\psi}}{\partial \bar{x}}\,. \tag{2.8}$$

The non-dimensional parameters are the Prandtl number

$$\sigma = \nu/\kappa \tag{2.9}$$

and the Rayleigh number

$$R = \beta g\,\Delta T'\,h^3/\nu\kappa\,. \tag{2.10}$$

The rigid end walls are impermeable and at constant temperature, so that

$$\bar{\psi} = \frac{\partial \bar{\psi}}{\partial \bar{x}} = \bar{T} = 0 \quad \text{on } \bar{x} = 0\,, \tag{2.11}$$

and

$$\bar{\psi} = \frac{\partial \bar{\psi}}{\partial \bar{x}} = 0\,, \qquad \bar{T} = 1 \quad \text{on } \bar{x} = L\,, \tag{2.12}$$

where

$$L = l/h \tag{2.13}$$

is the cavity aspect ratio. The horizontal walls are rigid and conducting, so that

$$\bar{\psi} = \frac{\partial \bar{\psi}}{\partial \bar{z}} = 0\,, \qquad \bar{T} = \frac{\bar{x}}{L} \quad \text{on } \bar{z} = 0, 1\,. \tag{2.14}$$

Gill [17] noted that the governing equations and boundary conditions possess the centrosymmetry properties

$$\begin{aligned} \bar{\psi}(\bar{x}, \bar{z}; L, R, \sigma) &= \bar{\psi}(L - \bar{x}, 1 - \bar{z}; L, R, \sigma)\,, \\ \bar{T}(\bar{x}, \bar{z}; L, R, \sigma) &= 1 - \bar{T}(L - \bar{x}, 1 - \bar{z}; L, R, \sigma)\,, \end{aligned} \tag{2.15}$$

which allows half the flow domain to be considered.

This work is concerned with the limit $L \to \infty$ such that

$$R_1 = R/L = \mathrm{O}(1) \tag{2.16}$$

for which the flow contains strong non-linear effects in end regions near the vertical walls.

3. Core region

Away from the ends of the cavity appropriate independent variables are

$$\xi = \bar{x}/L\,, \qquad z = \bar{z}\,. \tag{3.1}$$

Expanding formally the stream function and the temperature,

$$\begin{aligned}\bar{\psi}(\bar{x}, \bar{z}; R_1, L, \sigma) &= \bar{\psi}_0(\xi, z; R_1, \sigma) + L^{-1}\bar{\psi}_1(\xi, z; R_1, \sigma) + \mathrm{O}(L^{-2})\,,\\ \bar{T}(\bar{x}, \bar{z}; R_1, L, \sigma) &= \bar{T}_0(\xi, z; R_1, \sigma) + L^{-1}\bar{T}_1(\xi, z; R_1, \sigma) + \mathrm{O}(L^{-2})\,,\end{aligned} \tag{3.2}$$

and substituting into (2.7) gives at O(1),

$$\frac{\partial^4\bar{\psi}_0}{\partial z^4} - R_1\frac{\partial\bar{T}_0}{\partial\xi} = 0\,, \tag{3.3}$$

$$\frac{\partial^2\bar{T}_0}{\partial z^2} = 0\,. \tag{3.4}$$

The use of Gill's centrosymmetry relations and the boundary conditions (2.12) gives

$$\bar{T}_0 = \xi\,, \qquad \bar{\psi}_0 = \frac{R_1}{24}\,z^2(1-z)^2\,. \tag{3.5}$$

At $\mathrm{O}(L^{-1})$, using the expressions found for $\bar{T}_0$ and $\bar{\psi}_0$,

$$\frac{\partial^2\bar{T}_1}{\partial z^2} = \frac{R_1}{12}\,z(1-z)(1-2z)\,, \tag{3.6}$$

$$\frac{\partial^4\bar{\psi}_1}{\partial z^4} - R_1\frac{\partial\bar{T}_1}{\partial\xi} = 0\,. \tag{3.7}$$

Using the same conditions as above gives

$$\bar{\psi}_1 = 0\,, \qquad \bar{T}_1 = R_1\left(\frac{z^5}{120} - \frac{z^4}{48} + \frac{z^3}{72} - \frac{z}{720}\right). \tag{3.8}$$

Further terms associated with inverse powers of L in (3.2) are zero so that

$$\bar{\psi} = R_1F(z)\,, \qquad \bar{T} = \xi + L^{-1}R_1G(z) \tag{3.9}$$

to within corrections which are exponentially small as $L\to\infty$ (see Section 4) and where $F(z) = (z^2/24)(1-z)^2$ and

$$G(z) = \frac{z^5}{120} - \frac{z^4}{48} + \frac{z^3}{72} - \frac{z}{720}\,. \tag{3.10}$$

The results (3.9) are only valid if a consistent solution can be found in end-regions near each vertical wall. Regions in (R_1, σ) parameter space for which parallel core structures exist are determined in later sections.

4. End region

At each end of the cavity is an approximately square region in which the flow is turned. The flow has a structure near $\bar{x} = 0$ defined by

$$\bar{\psi}(\bar{x}, \bar{z}; R_1, L, \sigma) = \psi(x, z; R_1, \sigma) + \cdots ,$$
$$\bar{T}(\bar{x}, \bar{z}; R_1, L, \sigma) = L^{-1} T(x, z; R_1, \sigma) + \cdots , \tag{4.1}$$

where

$$x = \bar{x} , \qquad z = \bar{z} . \tag{4.2}$$

ψ and T satisfy (2.6) and (2.7) with (ψ, T, x, z, R_1) replacing $(\bar{\psi}, \bar{T}, \bar{x}, \bar{z}, R)$. Boundary conditions in this end region are

$$\psi = \frac{\partial \psi}{\partial x} = T = 0 \quad \text{on } x = 0 , \tag{4.3}$$

$$\psi = \frac{\partial \psi}{\partial z} = 0 , \qquad T = x \quad \text{on } z = 0, 1 . \tag{4.4}$$

The end region solution matches with the core solution given that ψ and T have the following limiting behaviours

$$\psi \sim R_1 F(z) + \mathrm{O}(e^{-\alpha x}) , \tag{4.5}$$

$$T \sim x + R_1 G(z) + \mathrm{O}(e^{-\alpha x}) , \tag{4.6}$$

as $x \to \infty$, where $\mathrm{Re}(\alpha) > 0$. The decaying parts of the stream function and temperature in (4.5) and (4.6) have the forms

$$\phi(z; R_1, \sigma) \exp(-\alpha(R_1, \sigma) x) , \qquad \theta(z; R_1, \sigma) \exp(-\alpha(R_1, \sigma) x) , \tag{4.7}$$

respectively, where ϕ, θ and α are determined by the sixth-order boundary value problem

$$\phi^{iv} + 2\alpha^2 \phi'' + \alpha^4 \phi + \alpha R_1 \theta = \alpha R_1 (F''' \phi - F'(\phi'' + \alpha^2 \phi))/\sigma , \tag{4.8}$$

$$\theta'' + \alpha^2 \theta - \phi' = \alpha R_1 (G' \phi - F' \theta) , \tag{4.9}$$

with

$$\theta = \phi = \phi' = 0 \quad \text{on } z = 0, 1 . \tag{4.10}$$

The decomposition (4.7) follows from the fact that the decaying parts of ψ and T satisfy a pair of linear equations whose coefficients depend only on z, implying that the dependence on x is of exponential form.

The forms in (4.7) will be generated by the conditions (4.3) so that the end region will have a solution consistent with the core region solution only if a triply infinite set of

eigenvalues α with $\mathrm{Re}(\alpha) > 0$ exists. If the eigenvalue $\alpha(R_1, \sigma)$ corresponds to the eigenfunctions $\phi(z; R_1, \sigma)$ and $\theta(z; R_1, \sigma)$, the boundary value problem implies that $-\alpha(R_1, \sigma)$ corresponds to $\phi(1 - z; R_1, \sigma)$ and $-\theta(z; R_1, \sigma)$. Also if α is complex then the complex conjugate $\alpha^*(R_1, \sigma)$ corresponds to $\phi^*(z; R_1, \sigma)$ and $\theta^*(z; R_1, \sigma)$. Attention can therefore be restricted to the first quadrant of the α plane.

The roots can be counted by reference to the structure at $R_1 = 0$, which is not dependent on the Prandtl number, and which has a triply infinite set of eigenvalues with $\mathrm{Re}(\alpha) > 0$. At $R_1 = 0$, (4.8) becomes

$$\phi^{iv} + 2\alpha^2\phi'' + \alpha^4\phi = 0 \tag{4.11}$$

with $\phi = \phi' = 0$ on $z = 0$, 1 and (4.9) becomes

$$\theta'' + \alpha^2\theta - \phi' = 0 \tag{4.12}$$

with $\theta = 0$ on $z = 0$, 1.

Equations (4.11) and (4.12) indicate that there are real eigenvalues defined by trivial solutions of (4.11), that is, $\phi \equiv 0$ for all α, and from (4.12)

$$\alpha = n\pi\,, \qquad \theta = \sin n\pi z\,, \quad n = 1, 2 \ldots . \tag{4.13}$$

Complex eigenvalues are found from the non-trivial solutions of (4.11) and occur in two non-combining even and odd groups

$$\phi = \sin \alpha z - \alpha z \cos \alpha z + (\alpha \cot \alpha - 1) z \sin \alpha z \tag{4.14}$$

where α is the solution of

$$\sin^2\alpha - \alpha^2 = 0\,. \tag{4.15}$$

The even eigenfunctions correspond to the solutions of $\sin \alpha + \alpha = 0$, tabulated by Robbins and Smith [25]

$$\alpha = 4.2124 + 2.2507\mathrm{i},\ 10.713 + 3.1032\mathrm{i}, \ldots, \tag{4.16}$$

and the odd ones to the solutions of $\sin \alpha - \alpha = 0$, tabulated by Hillman and Salzer [26]

$$\alpha = 7.4977 + 2.7687\mathrm{i},\ 13.900 + 3.3522\mathrm{i}, \ldots . \tag{4.17}$$

5. Numerical results

A fourth-order Runge–Kutta scheme with Newton iteration was used to solve the eigenvalue problem numerically. Solutions were calculated for fixed σ by incrementing R_1 using the value of α at the previous R_1 as an initial estimate. By use of this method the roots could be traced from the known values at $R_1 = 0$.

Figures 1 and 2 show the first branches of the real and complex eigenvalues for infinite Prandtl number; each branch maintains a positive real part for all values of R_1, which indicates that the end-region solution matches in a consistent manner to the core region solution. The decay of the real eigenvalues as $R_1 \to \infty$ indicates the expansion of the end region into the core at large R_1.

Figure 3 shows the first few branches of the real eigenvalues at various finite Prandtl numbers; for $\sigma = 1$ there is little change from the infinite Prandtl number case and for $\sigma = 0.1$ the decay of the eigenvalues as $R_1 \to \infty$ is still apparent.

Figure 4 shows the first complex branch at Prandtl numbers of 0.1 and 1.0. For the $\sigma = 0.1$ branch the real part of α becomes zero at a critical value of $R_1 = R_{1c}$ and the root bifurcates into two imaginary branches for $R_1 > R_{1c}$. This type of bifurcation occurs for $\sigma \leqslant \sigma_c \simeq 0.27$

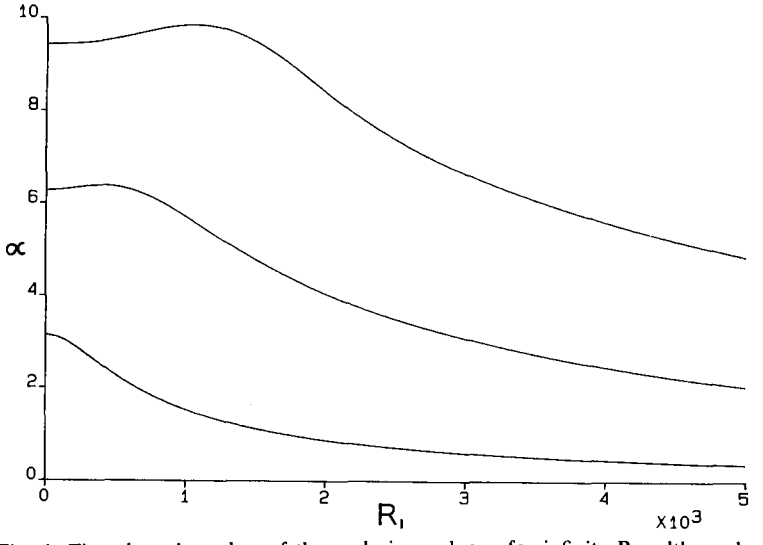

Fig. 1. First three branches of the real eigenvalue α for infinite Prandtl number.

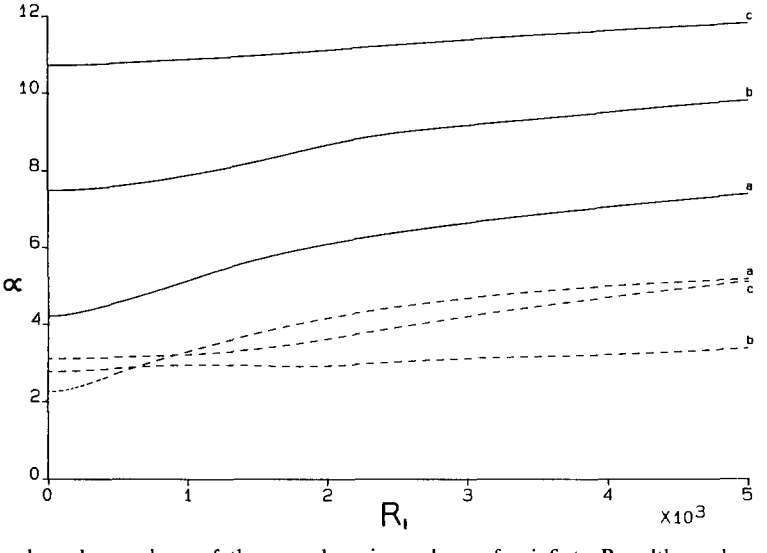

Fig. 2. First three branches a, b, c of the complex eigenvalue α for infinte Prandtl number, ——— real part, – – – – imaginary part.

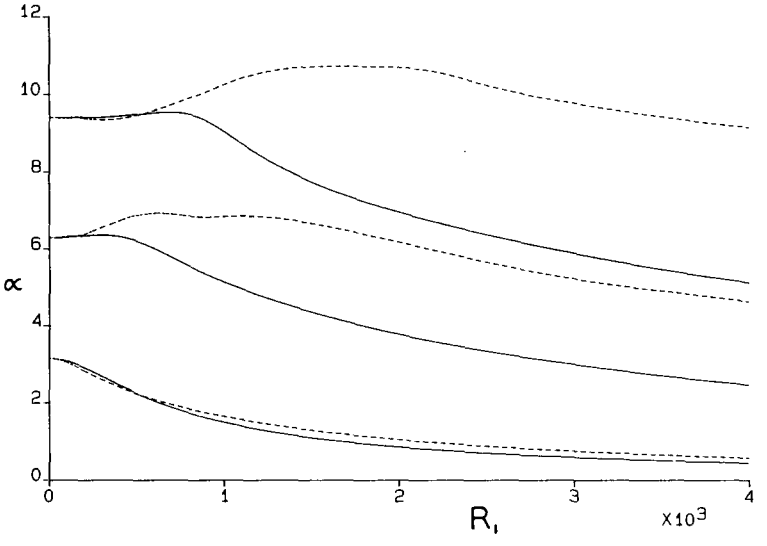

Fig. 3. First three branches of the real eigenvalue α for $\sigma = 0.1$, – – – –, and $\sigma = 1$, ———.

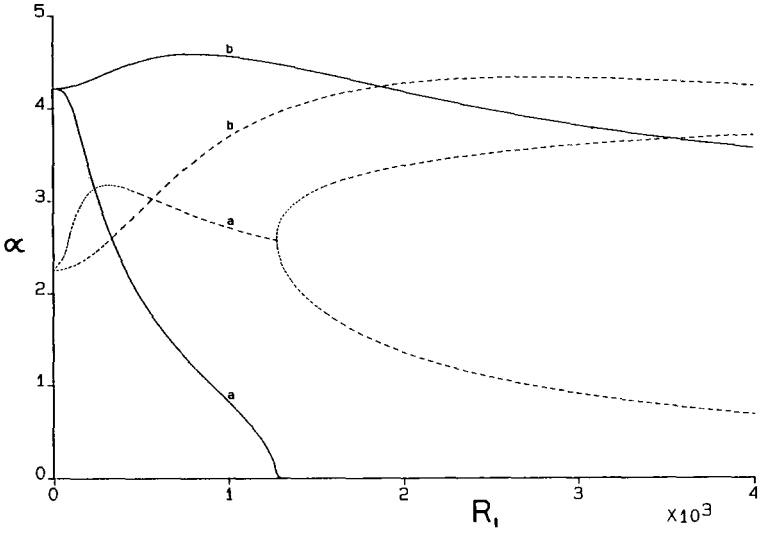

Fig. 4. Complex eigenvalues α for finite Prandtl number, ———, Real part, – – – –, Imaginary part; (a) $\sigma = 0.1$, (b) $\sigma = 1.0$.

with $\mathrm{Re}(\alpha)$ zero for $R_1 \geqslant R_{1c}(\sigma)$. Spatial oscillations from the end zone then enter the core and $R_{1c}(\sigma)$ may be identified with the critical Rayleigh number for the transverse mode of stationary instability of the parallel core flow, first examined by Hart [22]. Figure 5 shows the critical Grashof number

$$\mathrm{Gr}_c = R_{1c}/\sigma \tag{5.1}$$

as a function of σ.

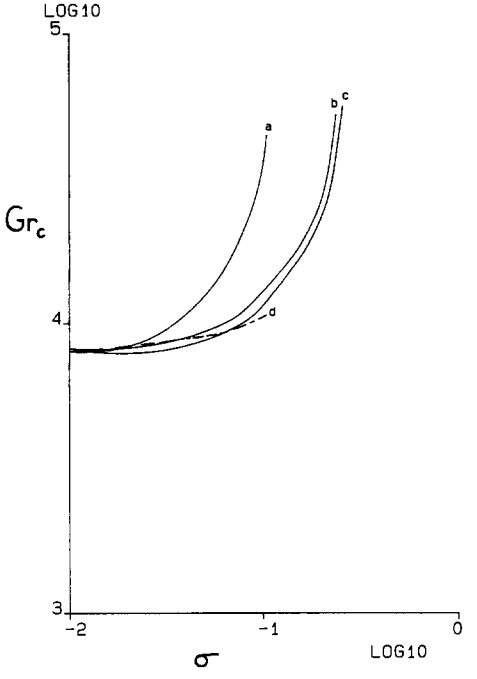

Fig. 5. Comparison of critical Grashof numbers: (a) Daniels et al. [24]. (b) Present work. (c) Kuo et al. [21]. (d) Hart [22].

6. Asymptotic results for large R_1

(*i*) *Decaying roots*

The real branches in Figs 1 and 3 have the asymptotic form

$$\alpha \sim \alpha_0/R_1 \quad \text{as } R_1 \to \infty\,, \tag{6.1}$$

where α_0 is the eigenvalue defined by the boundary value problem

$$\phi^{iv} + \alpha_0\theta = (\alpha_0/\sigma)(F'''\phi - F'\phi'')\,, \tag{6.2}$$

$$\theta'' - \phi' = \alpha_0(G'\phi - F'\theta)\,, \tag{6.3}$$

with

$$\phi = \phi' = \theta = 0 \quad \text{on } z = 0, 1\,. \tag{6.4}$$

Numerical solutions calculated by a Runge–Kutta scheme are shown in Fig. 6. Real solutions exist for all Prandtl numbers, and the leading branches approach the limiting values

$$\alpha_0 = 1852,\ 11052,\ 30919 \quad \text{as } \sigma \to \infty\,, \tag{6.5}$$

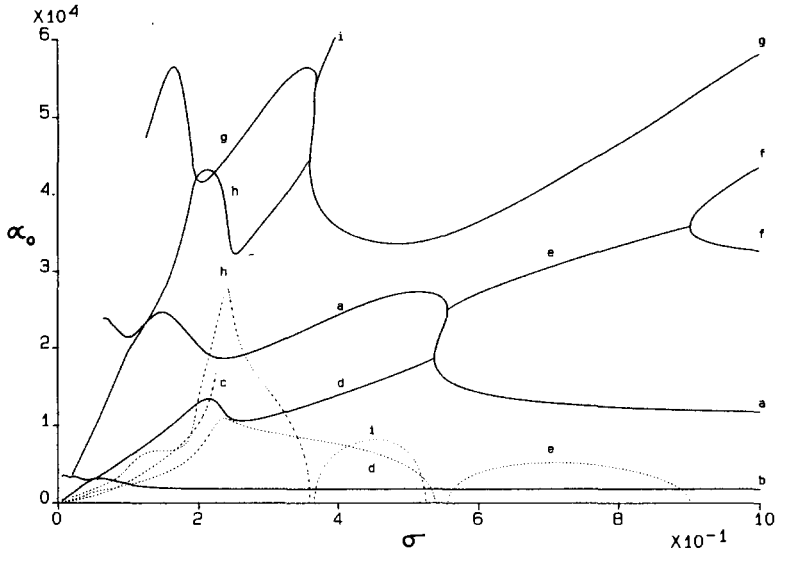

Fig. 6. Eigenvalues α_0 as a function of Prandtl number, ———, Real part, – – – –, Imaginary part.

found by taking the right-hand side of (6.2) equal to zero. Wholly imaginary roots exist for $\sigma < 0.24$.

(*ii*) *Finite roots*

Numerical calculations suggest that asymptotic solutions exist in which α remains finite as $R_1 \to \infty$ and purely imaginary solutions may correspond to the upper branches of the neutral curves in Fig. 4. For such solutions

$$\alpha \sim \mathrm{i}\bar{\alpha}\,, \qquad \phi \sim \bar{\phi}(z)\,, \qquad \theta \sim \bar{\theta}(z) \quad \text{as } R_1 \to \infty\,, \tag{6.6}$$

where $\bar{\alpha}$ is real. Substitution into (4.9) gives

$$\bar{\theta} = G'\bar{\phi}/F' \tag{6.7}$$

and therefore (4.8) yields

$$\bar{\phi}'' + ((\sigma G' - F'F''')/F'^2 - \bar{\alpha}^2)\bar{\phi} = 0\,. \tag{6.8}$$

A local solution of (4.8) and (4.9) consistent with (4.10), close to the lower surface of the cavity, requires that

$$\bar{\phi} = \mathrm{O}(z^{\lambda})\,, \qquad \bar{\theta} = \mathrm{O}(z^{\lambda-1}) \quad \text{as } z \to 0\,, \tag{6.9}$$

where $\lambda = \frac{1}{2}\{1 + (1 + \frac{4}{5}\sigma)^{1/2}\}$. It is also required that $\bar{\phi} = 0$ at $z = 1$. From (6.8) it can be shown that

$$\bar{\phi} \sim K_{\pm} \left| z - \frac{1}{2} \right|^{(1\pm\gamma)/2} \quad \text{as} \left| z - \frac{1}{2} \right| \to 0 , \tag{6.10}$$

where $K_{\pm}$ are arbitrary constants, and

$$\gamma = (1 - 14\sigma/5)^{1/2} . \tag{6.11}$$

It may be argued that for $\sigma < 5/14$ the stronger of the two singularities must be avoided i.e. $K_{-} = 0$. If the reverse were true then a solution subject to (6.9) would have to be constructed in $z < \frac{1}{2}$ with $K_{-} \neq 0$ and the symmetry of (6.8) implies a similar behaviour would occur in $z > \frac{1}{2}$. The structure near $z = \frac{1}{2}$ is then a critical layer defined by

$$z = \tfrac{1}{2} + (R_1 \bar{\alpha})^{-1/3} \tilde{z} , \tag{6.12}$$

$$\begin{aligned} \phi &\sim (R_1 \bar{\alpha})^{-(1/6)(1-\gamma)} \Phi(\tilde{z}) , \\ \theta &\sim (R_1 \bar{\alpha})^{(1/6)(1-\gamma)} \Theta(\tilde{z}) , \end{aligned} \tag{6.13}$$

where it is assumed that $\bar{\phi} = 0(1)$. Substitution back into (4.8) and (4.9) gives

$$576\sigma\Phi^{vi} - 24\mathrm{i}\tilde{z}(1+\sigma)\Phi^{iv} - 48\mathrm{i}\Phi''' - \tilde{z}^2\Phi'' - \frac{7\sigma}{10}\Phi = 0 , \tag{6.14}$$

which is independent of $\bar{\alpha}$. The solution of (6.14) must satisfy

$$\Phi \sim K_{-} |\tilde{z}|^{(1/2)(1-\gamma)} \quad \text{as} \ |\tilde{z}| \to \infty . \tag{6.15}$$

Daniels, Blythe and Simplins [24] considered a similar problem to (6.14) and (6.15) and were able to show that non-zero solutions would not generally exist, contradicting the original assertion and suggesting that the outer solution must satisfy

$$K_{-} = 0 . \tag{6.16}$$

Figure 7 shows the numerical solution of (6.8) subject to (6.9) and (6.16). To distinguish between the two singular forms in (6.10), the solution is rewritten as

$$\bar{\phi} = Z^{(1/2)(1-\gamma)} f(\zeta) \tag{6.17}$$

where

$$Z = \tfrac{1}{2} - z , \qquad \zeta = Z^{\gamma} , \tag{6.18}$$

$$f'' + \zeta^{2(1-\gamma)/\gamma} \gamma^{-2} \left\{ \frac{16(1-\gamma)^2(2\zeta^{2/\gamma} - 1)}{7(1 - 4\zeta^{2/\gamma})^2} + \frac{24}{(1 - 4\zeta^{2/\gamma})} - \bar{\alpha}^2 \right\} f = 0 . \tag{6.19}$$

The boundary conditions derived from (6.9) and (6.16) are

$$f = 0 \quad \text{at} \ \zeta = 0, \ 2^{-\gamma} . \tag{6.20}$$

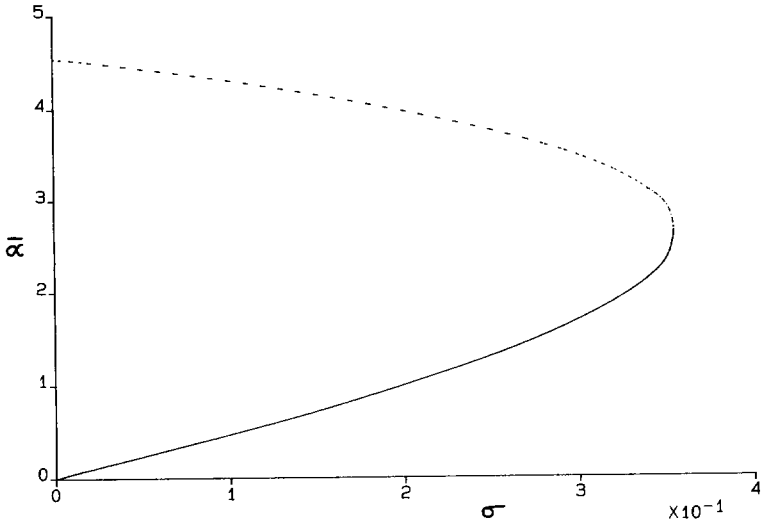

Fig. 7. Eigenvalues $\bar{\alpha}$ for $0 < \sigma < 5/14$.

The numerical solution was computed from $\zeta = 0$ to $\zeta = 2^{-\gamma}$ using an additional initial condition $f' = 1$ at $\zeta = 0$; iterative adjustment of $\bar{\alpha}$ enabled a solution to be found for any Prandtl number $0 < \sigma < 5/14$. The influence of the central singularity can be seen by replacing (6.16) by

$$K_+ = 0 . \tag{6.21}$$

The resulting upper branch of Fig. 7 is obtained by use of the conditions

$$f = 1 , \qquad f' = 0 \quad \text{at } \zeta = 0 , \qquad f = 0 \quad \text{at } \zeta = 2^{-\gamma} . \tag{6.22}$$

The form of the solution for $\bar{\alpha}$, on the lower branch of Fig. 7, can be found analytically for small Prandtl number, where

$$\bar{\alpha} \sim \sigma \bar{\alpha}_0 \quad \text{as } \sigma \to 0 . \tag{6.23}$$

The corresponding eigenfunction is

$$\bar{\phi} = \bar{\phi}_0 + \sigma \bar{\phi}_1 + \sigma^2 \bar{\phi}_2 + \cdots , \tag{6.24}$$

and substitution into (6.8) gives at leading order

$$F' \bar{\phi}_0'' - F''' \bar{\phi}_0 = 0 . \tag{6.25}$$

The boundary conditions on $\bar{\phi}_0$ obtained from (6.9) and (6.16) are

$$\bar{\phi}_0 = O(z) \quad \text{as } z \to 0 , \tag{6.26}$$

and

$$\bar{\phi}_0 \sim K_+ \left| z - \frac{1}{2} \right| \quad \text{as} \left| z - \frac{1}{2} \right| \to 0 \tag{6.27}$$

giving, without loss of generality,

$$\bar{\phi}_0 = F' \,. \tag{6.28}$$

At order σ,

$$F'\bar{\phi}_1'' + G' - F'''\bar{\phi}_1 = 0 \,, \tag{6.29}$$

and the boundary conditions on $\bar{\phi}_1$ are

$$\bar{\phi}_1 = \mathrm{O}(z \log_e z) \quad \text{as } z \to 0 \tag{6.30}$$

and

$$\bar{\phi}_1 \sim \frac{-7}{10} K_+ \left| z - \frac{1}{2} \right| \log_e \left| z - \frac{1}{2} \right| \quad \text{as} \left| z - \frac{1}{2} \right| \to 0 \,. \tag{6.31}$$

Writing

$$\bar{\phi}_1 = F'H(z) \,, \tag{6.32}$$

(6.29) reduces to

$$\frac{d}{dz}\left[F'^2 H'\right] = -G' \tag{6.33}$$

and use of (6.30) and (6.31) gives

$$H = \frac{1}{10} \log_e \frac{z^2(1-z)^2}{(\frac{1}{2} - z)^7} + \text{constant} \,. \tag{6.34}$$

At order σ^2,

$$F'^2\bar{\phi}_2'' + G'\bar{\phi}_1' - F'F'''\bar{\phi}_2 - F'^3\bar{\alpha}_0^2 = 0 \,, \tag{6.35}$$

and the boundary conditions on $\bar{\phi}_2$ are

$$\bar{\phi}_2 = \mathrm{O}(z \log_e^2 z) \quad \text{as } z \to 0 \tag{6.36}$$

and

$$\bar{\phi}_2 \sim \frac{1}{2}\left(\frac{7}{10}\right)^2 K_+ \left| z - \frac{1}{2} \right| \log_e^2 \left| z - \frac{1}{2} \right| \quad \text{as} \left| z - \frac{1}{2} \right| \to 0 \,. \tag{6.37}$$

A consistent solution of (6.35) exists only if

$$\int_0^{1/2} (\bar{\alpha}_0^2 F'^2 - G'H)\, \mathrm{d}z = 0 \,, \tag{6.38}$$

Table 1. Numerical solution of (6.19), (6.20) for small σ

σ	$\bar{\alpha}$	$\bar{\alpha}/\sigma$
0.20	0.98708	4.93542
0.15	0.71227	4.74846
0.10	0.46044	4.60443
0.05	0.22447	4.48946
0.01	0.04413	4.41296

Asymptotic $\bar{\alpha}/\sigma = 4.39545$.

which gives

$$\bar{\alpha}_0 = \frac{1}{5}\sqrt{483} \simeq 4.39545\,.$$

This result compares well with the numerical solution, as shown in Table 1 and Fig. 7.

7. Discussion

Convective motions driven by a horizontal temperature gradient in a shallow cavity with conducting walls have been analysed for the limit $L \to \infty$ with $R_1 = R/L = O(1)$, over a range of Rayleigh numbers R_1 and Prandtl numbers σ.

The numerical solution to the relevant eigenvalue problem indicates the existence of a critical Prandtl number $\sigma \simeq 0.27$ below which the parallel core flow is destroyed by multiple eddies which are forced into the core if the Grashof number $Gr = R_1/\sigma$ is greater than the critical value $Gr_c(\sigma)$ shown in Fig. 5. As $\sigma \to 0$ the results show that Gr_c approaches a value of about 8×10^3 consistent with, but a little higher than, the critical Grashof number of 7980 for $\sigma < 0.02$ found by Hart [22]. Figure 5 shows that the results also compare well with the work done by Kuo, Korpela, Chait and Marcus [21] whose stability analysis was based on the use of Chebychev polynomials and collocation. The insulating boundaries case was studied by Daniels, Blythe and Simpkins [24] and their results for the critical Grashof number as a function of Prandtl number are also included in Fig. 5. The Gr_c curves for the insulating and conducting boundaries approach the same limit as $\sigma \to 0$, consistent with Hart's [22] arguments that the critical Grashof number should be the same because the thermal contributions become negligible in this limit.

At general Prandtl number, the decay of the end zone solution is reduced as the Rayleigh number is increased, causing the structure set out in Sections 3 and 4 to break down. Figure 6 identifies the e-folding decay length

$$x \sim \alpha_0^{-1} R_1 \tag{7.1}$$

associated with this process, with $\alpha_0 \simeq 1.8 \times 10^3$ for $\sigma \geqslant 0.2$.

Acknowledgement

The author is grateful for help and encouragement from Professor P.G. Daniels and to the Science and Engineering Research Council for financial support in the form of a research studentship.

References

1. G. Hadley, Concerning the cause of the general trade winds, *Phil. Trans. R. Soc. Lond.* 39 (1735) 58–62.
2. H. Jeffreys, On fluid motion produced by differences of temperatures and humidity, *Q. Jl. R. met. Soc.* 51 (1925) 347–356.
3. A. Defant, *Physical oceanography*, Vol. 1, New York: Pergamon Press (1961).
4. M. Stern, *Ocean circulation physics*, New York: Academic Press (1975).
5. D.T.J. Hurle, Temperature oscillations in molten metals and their relationship to growth striae in melt-grown crystals, *Phil. Mag.* 13 (1966) 305–310.
6. D.T.J. Hurle, E. Jakeman and C.P. Johnson, Convective temperature oscillations in molten gallium, *J. Fluid Mech.* 64 (1974) 565–576.
7. A.E. Gill, A theory of thermal oscillations in liquid metals, *J. Fluid Mech.* 64 (1974) 577–588.
8. B.E. Boyack and D.W. Kearney, Heat transfer by laminar natural convection in low aspect ratio cavities, *ASME paper*, 72-HT-2 (1972).
9. D.E. Cormack, L.G. Leal and J. Imberger, Natural convection in a shallow cavity with differentially heated end walls, Part 1: Asymptotic theory, *J. Fluid Mech* 65 (1974) 209–229.
10. A. Bejan and A.N. Rossie, Natural convection in a horizontal duct connecting two fluid reservoirs, *J. Heat Transfer* 103 (1981) 108–113.
11. H.T. Rossby, On thermal convection driven by non-uniform heating from below: an experimental study, *Deep Sea Res.* 12 (1965) 9–16.
12. J. Imberger, Natural convection in a shallow cavity with differentially heated end walls, Part 3: Experimental Results, *J. Fluid Mech.* 65 (1974) 247–260.
13. S. Ostrach, R.R. Loka and A. Kumar, Natural convection in low aspect ratio rectangular enclosures, 19th Nat. Heat Transfer Conf. Orlando, *ASME Heat Transfer Division* 8 (1980) 1–10.
14. A. Bejan, A.A. Al-Hammoud and J. Imberger, Experimental study of high Rayleigh number convection in a horizontal cavity with different end temperatures, *J. Fluid Mech.* 109 (1981) 283–299.
15. P.G. Simpkins and T.D. Dudderar, Convection in rectangular cavities with differentially heated end walls, *J. Fluid Mech.* 110 (1981) 433–456.
16. P.G. Simpkins and K.S. Chen, Convection in horizontal cavities, *J. Fluid Mech.* 166 (1986) 21–39.
17. A.E. Gill, The boundary layer regime for convection in a rectangular cavity, *J. Fluid Mech.* 26 (1966) 515–536.
18. C. Quon, High Rayleigh number convection in an enclosure – a numerical study, *Physics of Fluids* 15 (1972) 12–19.
19. D.E. Cormack, L.G. Leal and J.H. Seinfeld, Natural convection in a shallow cavity with differentially heated end walls, Part 2: Numerical Solutions, *J. Fluid Mech.* 65 (1974) 231–246.
20. G.S. Shiralkar and C.L. Tien, A numerical study of laminar natural convection in shallow cavities, *J. Heat Transfer* 103 (1981) 226–231.
21. H.P. Kuo, S.A. Korpela, A. Chait and P.S. Marcus, *Eighth Intl. Heat Transfer Conf. San Francisco* 4 (1986) 1539.
22. J.E. Hart, Stability of thin non-rotating Hadley circulations, *J. Atmos. Sci.* 29 (1972) 687–697.
23. J.E. Hart, A note on the stability of low Prandtl number Hadley circulation, *J. Fluid Mech.* 132 (1983) 271–281.
24. P.G. Daniels, P.A. Blythe and P.G. Simpkins, Onset of multicellular convection in a shallow laterally heated cavity, *Proc. R. Soc. Lond.* A411 (1987) 327–350.
25. C.I. Robbins and R.C.T. Smith, A table of roots of $\sin z = -z$, *Phil. Mag.* 39 (1948) 1005.
26. A.P. Hillman and M.E. Salzer, Roots of $\sin z = z$, *Phil. Mag.* 34 (1943) 575.